

## Experiments in a floating water bridge

Jakob Woisetschläger

*Experimental Turbomachinery Research and Optical Measurement Group,  
Institute for Thermal Turbomachinery and Machine Dynamics, Graz University of  
Technology*

*Inffeldgasse 25 A, 8010 Graz, Austria*

Phone: +43 316 873 7277

Fax: +43 316 873 7239

e-mail: jakob.woisetschlaeger@tugraz.at

Karl Gatterer

*Institute of Physical and Theoretical Chemistry, Graz University of Technology  
Rechbauerstr. 12 A, 8010 Graz, Austria*

Phone: +43 316 873 8239

Fax: +43 316 873 108239

e-mail: gatterer@tugraz.at

Elmar C. Fuchs

*Wetsus - Centre of Excellence for Sustainable Water Technology  
Agora 1, 8900 CC Leeuwarden, The Netherlands*

Phone.: +31 58 28 46398

Fax.: +31 58 28 46202

e-mail: elmar.fuchs@wetsus.nl

**Abstract:** In a high-voltage direct-current experiment a watery connection formed between two beakers filled with deionised water, giving the impression of a ‘floating water bridge’. Having a few millimetres diameter and up to 2.5 centimetres length, this watery connection reveals a number of interesting phenomena currently discussed in water science. Focusing on optical measurement techniques the flow through the bridge was visualized and data were recorded such as flow velocity and directions, heat production, density fluctuations, pH values, drag force and mass transfer. To provide a better understanding of the basic phenomena involved, the discussion references related literature.

**Keywords:** optical measurement, water science, high voltage

## Introduction

In 1893 Sir William George Armstrong reported a remarkable direct-current high-voltage experiment to the Newcastle Literary and Philosophical Society: „Taking two wine-glasses filled to the brim with chemically pure water, I connected the two glasses by a cotton thread coiled up in one glass, and having its shorter end dipped into the other glass. On turning on the current, the coiled thread was rapidly drawn out of the glass containing it, and the whole thread deposited in the other, leaving, for a few seconds, a rope of water suspended between the lips of the two glasses.”(Armstrong 1893)

As gimmick from early days of electricity this experiment was handed down through history until the authors learned about it from W. Uhlig, ETH Zürich (Uhlig 2005). Although easy to reproduce, this watery connection between the two beakers holds a number of interesting static and dynamic phenomena. Heat and mass transfer can also be observed through this rope of water, further referred to as ‘floating water bridge’ shown in Fig.1 (Fuchs *et al.* 2007, Fuchs *et al.* 2008).

At macroscopic scale several of these phenomena can be explained by modern electrohydrodynamics, analyzing the motion of fluids in electric fields (e.g. Castellanos 1998), while on the molecular scale water can be described by quantum mechanics (e.g. Mrázek and Burda 2006; Jorgensen and Tirado-Rives 2005). The gap at mesoscopic scale is bridged by a number of theories including quantum mechanical entanglement and coherent structures in water, theories which are currently discussed (e.g. Del Giudice 2006; Head-Gordon and Johnson 2006; Stanley *et al.* 2005; Chatzidimitriou-Dreismann *et al.* 1997; Arani *et al.* 1995). These properties of water at mesoscopic scale have drawn special attention due to their importance to human physiology (Pollack 2001).

Experimentally these scales are also understood by optical measurement techniques, with most of them applicable to this experiment since the water cylinder forming between the two glass beakers floats in air freely. For all these reasons fully understanding this experiment might bridge the gap between our knowledge at mesoscopic scale and a future quantum-electrohydrodynamic theory of water.

## Experimental setup

For the experiments discussed two beakers with 60 mm diameter and 35 mm height made of glass or Teflon were filled with deionised water (Fig.2). Each glass beaker had a wall strength of 1.5 mm, a 2.2 – 2.5 mm (diameter) lip around the upper edge and a single spout. If not otherwise stated the beakers were filled with deionised water such that the water surface was about 3 mm below the beaker's edge. The initial conductivity of the deionised water was  $0.056 \mu\text{S cm}^{-1}$  recorded with the integrated conductivity meter of the Barnstead NANOpure type I ultrapure water system used (Thermo Fisher Scientific Inc., Waltham, MA), but rose quickly to  $0.8 \mu\text{S cm}^{-1}$  with a pH value of 5 due to  $\text{CO}_2$  saturation (see also Kendall 1916). For conductivity measurements, a WTW LF 91 was used, for pH value measurements a WTW ph 330i pH meter (both from WTW Wissenschaftlich-Technische Werkstätten GmbH, Weilheim, Germany). The WTW LF 91 conductivity meter was calibrated using a  $12.88 \mu\text{S cm}^{-1} \pm 1\%$  solution (KS910, Radiometer Analytical, Lyon, France) and had a measurement range from  $0.0 - 199.9 \mu\text{S cm}^{-1}$ , a temperature coefficient of  $2.1\% \text{K}^{-1}$  and an automatic temperature compensation from  $0 - 50^\circ \text{C}$ . The pH meter had a pH -2 to +19.99 range and a 0.005 pH digits accuracy ( $15 - 35^\circ \text{C}$ ). Alternatively, a universal indicator solution (No 36828, Riedel-de Haën GmbH, Seelze, Germany) with a pH 4 – 10 range was added to the water, raising the conductivity of this mixture to  $2.0 \mu\text{S cm}^{-1}$  (measured value at specified dilution). Using the indicator solution the pH was estimated by the color impression. This color impression gave only approximate pH values since the thickness of the layers observed changed within the cylindrical beakers. For visualization purposes small amounts of Rhodamine B (Merck 7599) predissolved in ethanol were added to the water in the beakers resulting in an overall conductivity of  $2.4 \mu\text{S cm}^{-1}$ .

For most of the experiments thin platinum plates were used as electrodes. These plates had a diameter of 32 mm with 0.5 mm thickness and were placed in the centre of the beakers. For single tests these platinum electrodes were exchanged by cylindrical silver or metal (nickel-plated) electrodes with 3.5 mm diameter. Depending on the position of the spout the distance between the electrodes was 60 to 80 mm. To our experience the position of the pouring spout did not influence the bridge formation. On the other hand the overall bridge length, measured from water to water surface was important. Starting the bridge at

the beaker spout results in the maximum bridge length in free air, so this setup was used for visualizations. Since the geometry of the spout might vary from beaker to beaker we started the bridge without spout (over the beaker's edge) whenever an absolute bridge length was needed for measurements. Therefore the bridge was started without spout for mass flow, temperature or force measurements. If not otherwise stated the experiments were performed in air. In all figures the anode beaker is at the right side of the image.

The power was provided by a Phywe 'Hochspannungs-Netzgerät 25kV' (No 13671.93, Göttingen, Phywe Systeme GmbH, Germany) with the direct-current output stable at 0.5 mA and the voltage continuously adaptable up to 25 kV with a waviness smaller than 0.05% and a 0.1 kV accuracy. A 42 nF ceramic capacitor was connected in parallel to the electrodes. (see Fig.2)

For flow visualizations a ceramic glass diffuser (50 x 50 cm, 5 mm thick) was placed behind the beakers, illuminated by a halogen lamp from behind. For the fringe projection technique applied, an equally spaced black grid with vertical lines 1.6 mm wide and 3.3 mm distance was mounted on top of the diffuser 40 mm behind the beakers' centre. For single experiments a linear polarizer was put on top of the diffuser instead. The polarizing filter with 400 mm diameter was fixed in a rotatable mount with an angular scale (Tiedemann GmbH, Garmisch-Partenkirchen, Germany). For these experiments a second polarizing filter was placed in front of the imaging device, its polarization direction perpendicular to the first filter. Whenever light changed its polarization direction by refraction or reflection at the bridge, this light passed through the second polarization filter, indicating regions with possible birefringence or Brewster angle reflections.

For imaging a Canon 300D with a Sigma 105mm 1:2.8 macro lens, a Panasonic 3CCD NV-DX100 camcorder with Raynox DCR-150 or Raynox DCR-250 conversion lenses, or a Photron FASTCAM SA1 high-speed camera with a Nikkor 60 mm 1:2.8 macro lens were used. All images were scaled. With this scaling and the above macro lenses the bridge diameter and length were measured within  $\pm 0.2$  mm accuracy ( $\pm 0.1$  mm at each side). Additional illumination was provided by a 300 mW multi-line Ar<sup>+</sup> laser (Ion Laser Technology, Salt Lake City, Utah).

Additional optical measurements were performed using an Inframetrics Model 760 Infrared Thermal Imaging Radiometer including a 20° IR lens and

ThermaGRAM software for surface temperature measurements (Inframetrics, North Billerica, MA). Since this type of thermal imager uses a single detector, the relative accuracy is better than  $\pm 0.1^\circ \text{C}$ , the absolute accuracy better than  $\pm 2^\circ \text{C}$ .

Alternatively flow velocities were recorded by a one-component Dantec Flow Lite laser Doppler anemometer with a 10 mW helium-neon-laser at 160 mm focal length, a Dantec 57N20 Burst Spectrum Analyser and Burstware Software (Dantec, Roskilde, Denmark), with an accuracy of about 1 % in velocity recording, assuming that the tracer particles used can follow the flow without lag. For all flow visualizations or measurements using tracer particles, small amounts of polyamide particles with a nominal diameter of 5  $\mu\text{m}$  (Dantec PSP-5) were added to the water in the beakers. Using an ultrasonic bath these particles were deagglomerated in 50 mL deionised water.

To measure the horizontal force exerted by the water bridge onto the beakers, the anode beaker was placed on a mercury bed and the cathode beaker was fixed from underneath. This ‘floating’ anode beaker was then connected via a thread to a spring balance Pesola 20030 (Pesola, Baar, Switzerland). The balance had a measurement range from 0 – 30 g and a 0.25 g accuracy. In this way a horizontal force was recorded for different bridge lengths with minimal friction between anode beaker and supporting platform.

To record the mass flow through the water bridge both beakers rested on electronic scales Kern EW 1500 2M each equipped with a serial interface (Kern, Balingen, Germany) with a measurement range of 0 – 1500 g and a 0.01 g accuracy.

## Results

For high-speed visualization of the water bridge formation a fringe projection technique was applied, contouring the surface by a parallel fringe pattern (Fig.3). A description of this technique for shape measurement can be found in recent works of Chen *et al.* (2008) or Chen *et al.* (2000). Here, this technique was used for visualization purpose only - the surface shape becomes evident from the distortion of the otherwise parallel line reflections. Without voltage applied, the surface was slightly curled due to vibrations and curved towards the beaker’s edge due to the hydrophobic Teflon surface (Fig.3a). When the high-voltage was applied, the surface towered towards the opposite beakers,

particularly in the anodic beaker (Fig.3.b). Finally, small water jets were ejected, with and without spark discharge (Figs. 3c,d), when the voltage exceeded approximately 15 kV. One of these jets eventually formed a watery connection (Fig.3e) which stabilized while increasing its diameter (Fig.3f). Through this water bridge a mass and heat transfer can be observed (see also Fuchs *et al.* 2007) and was now measured quantitatively. Fig.4 presents the results obtained with two scales underneath the beakers and simultaneous observation by a CCD camcorder and a thermographic imager. For the deionised water an emissivity value of 0.96 was assumed in order to calculate the temperature distribution on the surface. The chronological development of the mass flow recorded can be divided into three time intervals: In interval A the beakers were in close contact (0 mm bridge length). During this interval the watery connection heated up rapidly and a mass transfer of 280 mg/s from the anode to the cathode beaker was observed. After about 20 seconds the beakers were pushed apart, the bridge length was approximately 9 mm with 2.1 mm bridge diameter. In the following interval B the net mass flow from anode to cathode beaker was constant at 40 mg/s, while the bridge heated up significantly with most of the hot surface water streaming into the cathode beaker. After 3 minutes of operation the mass flow direction on the surface started to change, hot surface water streamed also into the anode beaker, probably due to the increased hydrostatic pressure between the two water levels. In this interval C the bridge diameter increased slightly but irregularly to 2.6 mm, with a slight asymmetry: the smallest diameter part of the bridge having the hottest temperature. With this bridge length and with the platinum electrodes the floating water bridge remained stable for hours with occasional changes of the direction of the mass flow. At beaker distances larger than 20 mm and/or due to contamination by dissolved ions the bridge tends to break rapidly, forming small droplets, forced by the electric field to fly towards the beakers.

At an ambient temperature of 22°C the temperature increase on the surface of the bridge was recorded for two different beaker distances. The result is presented in Fig.5. For this figure a thermographic imager recorded the temperature values by averaging over the bridge surface-where most of the energy is released. As can be seen, the floating water bridge responds to length change similarly to an ohmic resistor. Additionally, the horizontal force exerted by the water bridge was recorded for a bridge length from 0 to 15 mm (beaker distance).

Together with the voltage necessary to maintain the bridge, the force and the length are plotted in Fig. 6. For this force measurement the current was constant at 0.5 mA. A linear fit was applied to the voltage recordings, while a fourth order polynomial function was used to fit the force data.

It is important to note that all the measurements described in this work were recorded at room temperature (20°-22°C). When ice water was used instead, the bridge had a significantly smaller diameter.

For pH visualization, a pH sensitive dye was added to the water. The resultant pH distribution after approximately 20 minutes of operation is shown in Fig.7. Since the dye increased the conductivity of the mixture the bridge diameter became less than 2 mm. For clearer visibility of the pH dependent colors the electrodes were placed as far apart as possible. For an additional test series a third beaker was placed between the two original ones, with two bridges forming as shown in Fig.7b. Although the background screen was used for the white balance of the camera system, the color impression gives only approximate pH values, since a constant depth of 10 mm would have been necessary for precise pH measurements. Ultimately a layered structure became visible in the cathode beakers, with high pH values at the wrinkled surface of the cathode and nearly neutral pH along the water surface. On the other hand the pH value in the anode beaker increased slightly. When the level difference became too high water with high pH swashed from the cathode to the anode beaker without significant changes in the pH values. A closer look showed that water from the bridge with a low pH value curled along the surface of the cathode beaker towards the electrode. This impression was confirmed when small amounts of Rhodamine B were added to the deionised water in the anode beaker. The water with Rhodamine B rapidly moved through the bridge, curling close underneath the water surface towards the cathode. To test for the influence of dye itself on the formation and operation of the bridge, in a separate experiment the pH dye was added only after 20 min of operation. Again the average pH value in the cathode beaker increased, while in the anode beaker it decreased slightly.

When tracer particles were added for flow measurements using a laser Doppler anemometer and for visualization, the floating water bridge revealed a rotating outer layer, made visible in Fig.8 by particle tracks. Details on these measurement techniques can be found in the books by Merzkirch (1987) and

Albrecht *et al.* (2003). Recorded by the laser Doppler anemometer a tangential velocity of approximately 0.3 m/s was found at mid-length, the axial velocities changed between  $\pm 0.2$  m/s, depending on the main direction of mass transfer in the outer layer towards the cathode or the anode beaker. For Fig.8 eight consecutive images recorded with a frame rate of 1 kHz were added, revealing similar tangential velocities as recorded by the laser Doppler anemometer. Even without tracer particles the rotation of the outer shell was observed with the high speed camera. Occasionally, single tiny gas bubbles crossed the bridge, rotating with the same speed as the tracer particles.

In a next experiment the water bridge was placed between two crossed polarizer plates diffusely illuminated from behind. In this arrangement some of the light passing through the bridge changed the polarization direction (Fig. 9a,b). Additionally, polarized reflections from the surfaces were observed. Due to the imaging properties of the water cylinder, the ceramic glass diffuser is imaged upside down through the bridge. When the diffuser with the polarizer plate on top was covered from above, the upper reflection on the water surface and the lower band of light in the bridge vanished first. In this way the reflection on the water surface was separated from the refraction through the bridge. Polarized reflections were seen since some of the diffuse light (linear polarized under  $-45^\circ$ ) reflected at the surface of the bridge at Brewster angle. This type of reflection removed the polarization component perpendicular to the water surface, the component parallel to the axis of the bridge then passed the analyzer plate ( $45^\circ$ ) partly. For the light refracted by the bridge the polarization effect observed could be caused by the same effect on the gas/water interfaces in a bubble network or by birefringence of the water in the outer layer. To test these possibilities a laser beam was focused into the bridge. This beam was guided along the inner surface of the bridge, similar to the way an optical fiber would guide the beam (Fig. 9c). A strong scatter was observed only in the outer layer of the bridge, supporting the bubble hypothesis. This experiment was repeated with degassed water used for the water bridge formation, but the same effects were observed. A detailed analysis of the scatter properties of small droplets and particles can be found in Albrecht *et al.* (2003) and Naqwi and Durst (1991).

In a next step, the diffuser plate was covered with vertical gridlines and these gridlines were imaged through the bridge. When vertical lines were imaged

through the water bridge, these lines were distorted due to different optical path lengths for the light rays refracted through the bridge (see Fig. 10). These changes in optical path can be due to geometrical changes (bridge diameter, surface waves) or to changes in the refractive index of the bridge. The deflection magnitude becomes evident from the distortions of the otherwise parallel gridlines. This technique is also used for schlieren visualization, displaying density gradients in compressible fluid flows (Settles 2001). Hence, the thickness of the water column and local density changes inside the water bridge were monitored simultaneously with the high speed camera at 5000 fps with every 20<sup>th</sup> frame displayed in Fig.10. Previous research (Fuchs *et al.*, 2007) used a schlieren technique to visualize strong gradients in the bridge. Using deflected grid lines as presented in Fig.10, it becomes evident that the change in deflection magnitude during very short time scales and for small distances is significant and cannot be explained only by surface waves (geometrical changes), which otherwise would become visible along the surface of the bridge. On the other hand, local density changes caused by a bubble network could easily account for such large deflections within a few millimeters distance.

Finally, the floating water bridge was exposed to additional magnetic and electrostatic fields. With a Neodymium magnet a slight cooling effect ( $\sim 5\text{ }^{\circ}\text{C}$ ) of the bridge was detected when the magnet was brought in close distance ( $\sim 2\text{ mm}$ ) of the bridge. However, this effect is solely due to the distortion of the electric field by the material of the magnet, since it was easily reproduced with a nonmagnetic piece of metal having the same dimensions.

On the other hand, a charged glass rod deflected the bridge due to dielectrophoresis, the motion of matter caused by alignment of polar molecules in a non-uniform electric field. Fig.11 demonstrates this effect with the water bridge. By bringing the charged glass rod closer to the bridge, first the outer layer was distorted and shed off in tangential direction (Fig.11 a), confirming the laser Doppler anemometer measurements which indicated a tangential velocity component in the outer shell of the bridge. With or without contact to the glass rod, the core of the bridge then decayed into a series of small droplets moving towards the electrodes still with a velocity component in axial direction (Fig.11 b).

## Discussion

The bridge formation described in the last section (Fig. 3) resembles the formation of electrohydrodynamic sprays or jets reviewed by Grace and Marijnissen (1994) or Eggers and Villermaux (2008). When the voltage applied exceeded a certain threshold, the water surfaces were lifted towards each other, with cones forming in both beakers. These cones have been described by Taylor (1964) (Taylor cones) and the phenomenon of dielectric liquids being pulled up in the vicinity of electrodes in high voltage fields has been discussed by Daba (1972) (Sumoto effect) and is currently used in devices for electrohydrodynamical pumping (e.g. Ohyama *et al.* 2005). The strong electric field induces free charges in the water surface, and as a result, electric stresses occur in this surface forming small cone jets. At higher voltages these cone jets break up into highly charged droplets (Hartman *et al.* 1999), in our experiment sometimes accompanied by discharges. Since these droplets carry charge, they disturb the electric field followed up by a disruption in the production of further jets from the water surface these droplets left behind. During this process the water surface impresses the observer by its highly tumultuous appearance (Fig.3d). Additionally, single ions escape the surface forming an ionic wind. This wind curls the charged water surface (Fig.3e). In our experiment, occasionally single jets formed a watery connection between the two water surfaces. With this contact, conduction and fluid flow started, accompanied by a voltage decrease from 15kV to 8 or 9kV, together with a significant increase in diameter of the water rope bridging the gap between the two beakers (Fig.3f). A possible explanation for this stabilization of the jet is the formation of the outer rotating shell (Fig.8). A detailed description of cone jets and their formation is given by Gañán-Calvo (1997).

The rotation of the outer shell of the bridge can be explained by electric shear forces induced in a slightly conducting liquid, when the surface supports surface charges together with an electric DC-field tangential to the surface (Melchor and Taylor 1969). A cellular flow pattern along the surface will form, which becomes visible in Fig.8 at the cathode beaker spout with a counter-clockwise rotation when observed from above. This cellular pattern would induce the observed rotation along the bridge surface.

As soon as the watery connection stabilized a horizontal force between the beakers was recorded (Fig.6). With a bridge length of 10 mm and a bridge

diameter of 2.2 mm the volume of this water column and the gravitational force acting on it was estimated assuming an overall density of  $998 \text{ kg/m}^3$ . At this length the horizontal drag force (Fig.6) exerted on the water molecules and ions is one order of magnitude higher than the gravitational force acting on the water column. Both forces result in the catenary's shape of the water bridge (Fig.1).

In this water bridge, forming between the two beakers, the main flow direction was from the anode to the cathode beaker. Assuming a mass transport of  $40 \text{ mg/s}$  (Fig.5, time interval B), a current of  $0.5 \text{ mA}$  and a density of  $998 \text{ kg/m}^3$ , with each positive charge a water volume equivalent to a sphere  $30 \text{ nm}$  in diameter would be transported. But, this first estimation does not consider that the charge density could be much higher if negative ions with a smaller solvation shell would counteract this effect. The high mobility of the hydrated protons  $\text{H}^+$  and the hydroxide ions  $\text{OH}^-$  in water and their complex differences have preoccupied scientists for decades (e.g. Tuckerman *et al.* 2002; Hynes 1999; Marx *et al.* 1999).

Previous experiments in a controlled atmosphere have shown that this water bridge forms well in air, nitrogen and oxygen, but not in helium or carbon-dioxide (Fuchs *et. al.* 2008). This is due to the increase in conductivity up to  $11.0 \mu\text{S cm}^{-1}$  caused by these gases being dissolved in water. This effect can be measured immediately after the bridge is shut off, with the values returning to normal a few minutes later in the case of Helium, and taking considerably more time to revert in the case of  $\text{CO}_2$ . In this previous work it was also observed that the conductivity increased when silver or aluminium electrodes were used due to electrolysis. It was found that at the given maximum current of  $0.5 \text{ mA}$  and maximum voltage of  $25 \text{ kV}$  the bridge will rupture at approximately  $10.0 \mu\text{S cm}^{-1}$ . Under helium atmosphere a glow discharge was preferred to the formation of a watery connection. With platinum electrodes under normal atmosphere no electrolysis and no increase in conductivity were observed, the water bridge was stable for hours. A possible explanation for the increased availability of hydrated protons and hydroxide ions is the dependence of the dissociation constant on the electric field in dielectric liquids discussed by Castellanos 1998 (Onsager's theory). A quantum chemical description of autoionization in water has been given by Geissler *et al.* (2001) who considered electric field fluctuations as

driving force for the dissociation of oxygen-hydrogen bonds even when water is not exposed to external electric fields.

It is widely accepted that water molecules form tetrahedral hydrogen-bonded structures, but the existence of strongly hydrogen-bonded chains or rings in a weakly hydrogen-bonded disordered network is still under discussion (Head-Gordon and Johnson 2006). It has also been discussed by Rai et. al. (2008) how an external electrical field smoothes the three-dimensional structures, eventually breaking up the structures, forming a linear or net-like structure of hydrogen-bonded molecules. Looking at the heat production on the surface of the water rope bridging the two beakers, it becomes evident that this volume is the electrohydrodynamic ‘bottleneck’ of the system, with increased resistance to current and fluid flow. The authors also hypothesize that this is the section in which most of the molecular rearrangements take place. So, this section must influence the proton transport significantly. The effect of electric fields on the proton transport through water chains has been discussed by Hassan *et al.* (2006), a general review on proton-transfer through hydrogen-bonded networks has been given by Marx (2006).

On the other hand, the visualization of the pH values in the two beakers indicate space-charge injection effects in the vicinity of the slightly rippled surface of the electrodes. Such effects in highly purified water have been visualized by Zahn and Takeda (1983), Klimov and Pollack (2007) and have been described by Froud and Gallagher (1996). The coulombic force on net space charges give rise to fluid motion and a layered structure in the vicinity of the electrodes. These charges also influence the electric field in the beakers, again focusing field effects on the bridge region. It might be interesting to note that the mass measurements revealed a mass transfer of 16 mg/s from the anode to the cathode beaker in case of the water/pH dye mixture ( $2.0 \mu\text{S cm}^{-1}$ , 0.5 mA) and the beaker dimensions used. Using the pH dye, the backflow happened only occasionally for no longer than approximately 25s, shortly before the water in the cathode beaker brimmed over. The pH of the bridge was difficult to estimate because of its small diameter. The dominant color was red, indicating a  $\text{pH} \leq 5$  for most parts of the bridge.

In the light of the results presented, the water bridge reveals a multi-layered structure with mass transport mainly from the anode to the cathode

beaker, a backflow preventing the cathodic beaker from overflowing thereby stabilizing the phenomenon for hours, and a rotating outer shell causing optical polarization effects. These polarization effects could be caused by electrically enforced birefringence in the outer layer, commonly known as the electro-optical Kerr effect. But due to the small Kerr constant of water the high-voltage field strength used for the floating water bridge is too low to observe a Kerr effect (e.g. Zahn and Takada, 1983). Therefore scatter from micrometer-sized bubbles, slightly elongated in the electric field seems more likely. Beside the polarization effects such bubbles could also explain the density changes observed. Nano-scaled coherent domains in water, postulated by Del Giudice 2006, could also cause density changes, but these domains would be too small to scatter light with intensities large enough to be observed in polarized light.

It has been reported by Krasucki (1966) that micro-bubbles can form in dielectric liquids when sufficiently high electric fields are applied, starting with vacuous cavities and vaporization of the liquid. These vapor bubbles will grow until electric breakdown is initiated. The presence of submicroscopic impurities in the water or gas pockets at the electrodes may trigger these points of zero pressure in the liquid. Micro-bubble phenomena in lubricated films induced by external electric fields have also been studied by Xie *et al.* (2008), giving a quantitative estimation for the formation of nano- and micro-sized bubbles in water and aqueous solutions together with the significant heat development inside these bubbles. The temperature rise at the bridge surface might be an additional indication for the formation of bubble-networks inside the bridge, additionally counter-acting surface tension. When the electric field through the bridge was distorted by a piece of metal brought close to the bridge, the bridge surface cooled down and became unstable with a rippled surface. This observation was possibly caused by a too low field strength inside to bridge due to the field distortion accompanied by a disruption in bubble production.

Additional weight was added to the bubble hypothesis in a recent neutron scattering study performed on a D<sub>2</sub>O water bridge (Fuchs *et al.* 2009). On the other hand Jin *et al.* (2007) report on the difficulties to distinguish between supramolecular structures and stable nano-bubbles in aqueous solutions. To reveal the structure of a possible bubble network in the water bridge and relate it to well understood experiments in other areas (e.g. sonochemistry, sonoluminescence,

electrification of cavitation bubbles and the relation between water pH value and bubble surface charge; Suslick and Flannigan 2008; Prevenslik 1998; Margulis and Margulis 2007; Elmahdy *et al.* 2008) further experiments in a floating water bridge have to be performed.

## Conclusions

A stable watery connection of several millimeter length formed when a high DC-voltage was applied to two beakers filled with deionized water. This centuries old experiment provides a stable environment to investigate a number of phenomena addressed in modern water science. The bridge formation resembles the formation of electrohydrodynamic sprays or jets, with a rotation of the outer layer of the bridge likely to be caused by electric shear forces. With platinum electrodes and no electrolysis observed, a relatively high current and mass flow was measured, with local variations of pH values in the beakers. The influence of the electric field on dissociation and / or the formation of nano-cavities in the water under normal atmosphere might cause these effects. The horizontal drag force inside the bridge and the gravitational force onto the water cylinder is responsible for its catenary's shape. The polarization effects observed are likely caused by micro-sized bubbles in the outer layer. The formation of a mesoscopic network of small structures (e.g. nano- or microbubbles) could possibly counteract the surface tension, heat up the bridge and contribute to the strong density changes observed. To finally decide which structures stabilize the bridge, additional experiments in the floating water bridge will be conducted.

## Acknowledgements

The authors gratefully acknowledge the support by the Institute of Analytical Chemistry and Food Chemistry, as well as by the Institute of Hydraulic Engineering and Water Resources Management, both at Graz University of Technology, for sharing the NANOpure system and the Photron high speed camera, respectively, and the support by H. Eisenkölbl (Graz University of Technology). With great pleasure the authors wish to thank Professors Cees Buisman (Wetsus – Centre of Excellence for Sustainable Water Technology), Emilio Del Giudice (University of Milano), Franz Heitmeir (Graz University of Technology), Jan C.M. Marijnissen (Delft University of Technology) and Gerald H. Pollack (University of Washington) for the ongoing discussion on the water bridge phenomenon (in alphabetic order).

## References

- Albrecht H-E, Borys M, Damaschke N, Tropea C (2003) *Laser Doppler and Phase Doppler Measurement Techniques*, Springer-Verlag Berlin Heidelberg New York, ISBN 3-540-67838-7
- Arani R, Bono I, Del Giudice E, Preparata G (1995) QED coherence and the thermodynamics of water, *International Journal of Modern Physics B*, 9:1813-1841
- Armstrong W G (1893) *The Newcastle Literary and Philosophical Society, The Electrical Engineer*, Feb. 10:154-155
- Castellanos A, Ed. (1998) *Electrohydrodynamics*, International Centre for Mechanical Sciences, CISM Courses and Lectures No.380, Springer, Wien, New York, ISBN 3-211-83137-1
- Chatzidimitriou-Dreisemann C A, Redah T A, Streffer R M F, Mayers J (1997) Anomalous Deep Inelastic Neutron Scattering from Liquid H<sub>2</sub>O-D<sub>2</sub>O: Evidence of Nuclear Quantum Entanglement, *Phys. Rev. Lett.* 79: 2839-2842. doi: 10.1103/PhysRevLett.79.2839
- Chen F, Brown GM, Song M (2000) Overview of three-dimensional shape measurement using optical method, *Opt. Eng.* 39:10-22. doi:10.1117/1.602438
- Chen XB, Xi JT, Jiang T, Jin Y (2008) Research and development of an accurate 3D shape measurement system based on fringe projection: Model analysis and performance evaluation, *Precision Engineering* 32: 215-221. doi:10.1016/j.precisioneng.2007.08.008
- Daba D (1972) The interpretation of the effect of climbing up electrodes of the dielectric liquids in stationary fields (the Sumoto effect), *J. Phys. A: Gen. Phys.* 5:318-326. doi: 10.1088/0305-4470/5/2/013
- Del Giudice E (2006) Old and new views on the structure of matter and the special case of living matter, *Journal of Physics: Conference Series* 67: 012006. doi:10.1088/1742-6596/67/1/012006
- Eggers J, Villermaux E (2008) Physics of liquid jets, *Rep. Prog. Phys.* 71: 036601. doi:10.1088/0034-4885/71/3/036601
- Elmahdy AM, Mirnezami M, Finch JA (2008) Zeta potential of air bubbles in presence of frothers, *International Journal of Mineral Processing* 89:40-43, doi:10.1016/j.minpro.2008.09.003
- Frood DG, Gallagher TJ (2006) Space-charge dielectric properties of water and aqueous electrolytes, *Journal of Molecular Liquids* 69:183-200. DOI: 10.1016/S0167-7322(96)90013-6
- Fuchs E C, Woisetschläger J, Gatterer K, Maier E, Pecnik R, Holler G, Eisenkölbl H (2007) The floating water bridge, *J. Phys. D: Appl. Phys.* 40: 6112-6114. doi: 10.1088/0022-3727/40/19/052
- Fuchs E C, Gatterer K, Holler G, Woisetschläger J (2008) Dynamics of the floating water bridge, *J. Phys. D: Appl. Phys.* 41: 185502 (5pp). doi: 10.1088/0022-3727/41/18/185502
- Fuchs E C, Bitschnau B, Woisetschläger J, Maier E, Beuneu B, Teixeira J (2009) Neutron scattering of a floating heavy water bridge, *J. Phys. D:Appl. Phys.* 42: 065502. doi: 10.1088/0022-3727/42/6/065502
- Gañán-Calvo A M (1997) On the theory of electrohydrodynamically driven capillary jets, *J. Fluid Mech.* 335: 165–188
- Geissler P L, Dellago C, Chandler D, Hutter J, Parrinello M (2001) Autoionization in liquid water, *Science* 291: 2121–2124. doi: 10.1126/science.1056991
- Grace JM, Marijnissen JCM (1994) A review of liquid atomization by electrical means, *J. Aerosol Sci.* 25:1005-1019. doi:10.1016/0021-8502(94)90198-8
- Jin F, Ye J, Hong LZ, Lam HF, Wu C (2007) Slow relaxation mode in mixtures of water and organic molecules: Supramolecular structures or nanobubbles?, *Journal of Physical Chemistry B* 111 (9):2255-2261, DOI: 10.1021/jp068665w
- Hartman R P A, Brunner D J, Camelot D M A, Marijnissen J C M, Scarlett B (1999) Electrohydrodynamic atomization in the cone-jet mode physical modelling of the liquid cone and jet, *J. Aerosol Sci.* 30 823–49. doi:10.1016/S0021-8502(99)00033-6
- Hassan SA, Hummer G, Lee YS (2006) Effects of electric fields on proton transport through water chains, *J Chem Phys.* 124:204510. DOI:10.1063/1.2198820
- Head-Gordon T, Johnson M E (2006) Tetrahedral structure or chains for liquid water, *Proc Natl Acad Sci USA* 21: 7973-7977. doi: 10.1073/pnas.0608020103
- Hynes JT (1999) The protean proton in water, *Nature* 397:565-567. doi:10.1038/17487

- Jorgensen W L, Tirado-Rives J (2005) Potential energy function for atomic-level simulations of water and organic and biomolecular systems, *Proc Natl Acad Sci USA*, 102: 6685-6670. doi: 10.1073/pnas.0408037102
- Kendall J (1916) The specific conductivity of pure water in equilibrium with atmospheric carbon dioxide, *J Am Chem Soc*, 38: 1480-1497
- Klimov A, Pollack GH (2007) Visualization of charge-carrier propagation in water, *Langmuir* 23:11890-11895. doi: 10.1021/la701742v
- Krasucki F (1966) Breakdown of liquid dielectrics, *Proc. Roy. Soc. A*294:393-404
- Marx D (2006) Proton transfer 200 years after von Grotthuss: Insights from ab initio simulations, *Chem. Phys.Chem.* 7:1848-1872. DOI: 10.1002/cphc.200600128
- Marx D, Tuckerman ME, Hutter J, Parrinello M (1999) The nature of the hydrated excess proton in water, *Nature* 397:601-602. doi: 10.1038/17579
- Margulis MA, Margulis IM (2007) Current State of the Theory of Local Electrification of Cavitation Bubbles, *Russian Journal of Physical Chemistry A*, 81:129–138 , doi:10.1134/S0036024407010232
- Melcher J R, Taylor G I (1969) Electrohydrodynamics: A Review of the Role of Interfacial Shear Stresses, *Annu Rev Fluid Mech*, 1: 111-146, doi:10.1146/annurev.fl.01.010169.000551
- Merzkirch W (1987) *Flow Visualization*, 2<sup>nd</sup> Ed., Academic Press, Orlando, ISBN 0-12-491351-2
- Mrázek J, Burda J V (2006) Can the pH value of water solutions be estimated by quantum mechanical calculations of small water clusters ?, *J. Chem. Phys.* 125: 194518. doi: 10.1063/1.2363383
- Naqwi AA, Durst F (1991) Light Scattering Applied to LDA and PDA Measurements Part 1: Theory and Numerical Treatment, *Part. Part. Syst. Charact.* 8: 245-258
- Ohyama R, Kumeta M, Ueda A, Watson A, Chang JS (2005) A fundamental characteristic and image analysis of liquid flow in an AW type EHD pump, *Journal of Visualization*, 8:339-346
- Pollack G H (2001) *Cells, Gels and the Engine of Life*, Ebener & Sons, Seattle WA, USA, ISBN 0-9626895-2-1
- Prevenslik TV (1998) Dielectric polarization in the Planck theory of sonoluminescence, *Ultrasonics Sonochemistry* 5 (3): 93-105, doi:10.1016/S1350-4177(98)00016-9
- Rai D, Kulkarni AD, Pathak RK (2006) Water clusters (H<sub>2</sub>O)<sub>n</sub>, n=6-8, in external electric fields, *J Chem. Phys.* 128:034310. doi: 10.1063/1.2816565
- Settles GS (2001) *Schlieren and Shadowgraph Techniques*, Springer, Berlin Heidelberg New York, ISBN 3-540-66155-7
- Stanley H E, Buldyrev S V, Franzese G, Giovambattista N, Starr F W (2005) Static and dynamic heterogeneities in water, *Phil. Trans. R. Soc. A* 363: 509-523. doi:10.1098/rsta.2004.1505
- Suslick KS, Flannigan DJ (2008) Inside a collapsing bubble: Sonoluminescence and the conditions during cavitation, *Annual Review of Physical Chemistry* 59:659-683, doi:10.1146/annurev.physchem.59.032607.093739
- Taylor F R S (1964) Disintegration of water drops in an electric field, *Proc. R. Soc. Lond. A*, *Math. Phys. Sci.* 280:383-397
- Tuckerman ME; Marx D; Parrinello M (2002) The nature and transport mechanism of hydrated hydroxide ions in aqueous solution, *Nature* 417:925-929. doi:10.1038/nature00797
- Uhlig W (2005) Personal communication, Laboratory of Inorganic Chemistry, ETH Hönggerberg – HCI, CH-8093 Zürich
- Xie GX , Luo JB , Liu SH, Zhang CH, Lu XC(2008) Micro-Bubble Phenomenon in Nanoscale Water-based Lubricating Film Induced by External Electric Field, *Tribol. Lett.* 29:169-176. doi 10.1007/s11249-007-9288-8
- Zahn M, Takada T (1983) High voltage electric field and space-charge distributions in highly purified water, *J. App. Phys.* 54:4762-4775. DOI:10.1063/1.332810

## Figures with captions

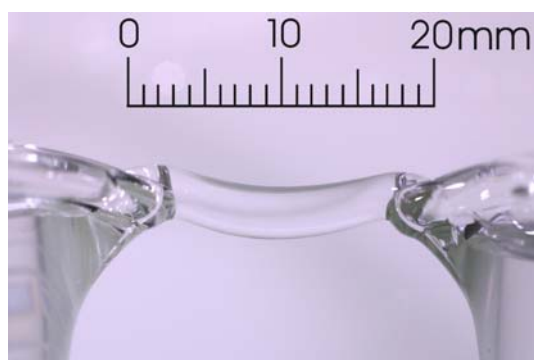


**Fig.1** Between two glass beakers filled with deionised water a watery connection forms when a high voltage is applied (referred to as ‘floating water bridge’).

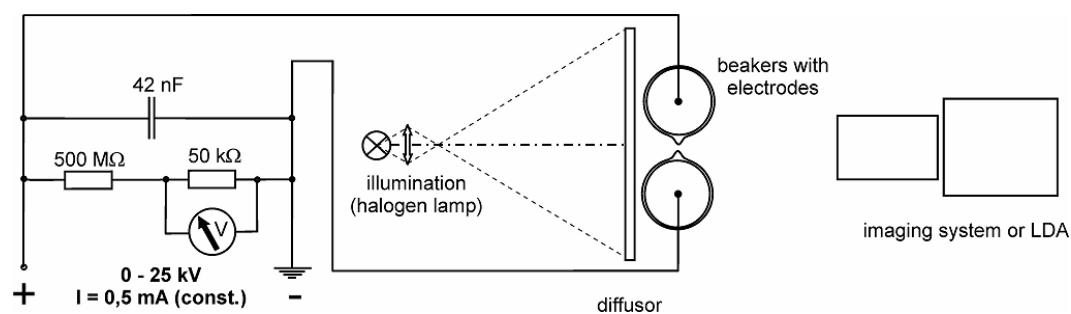


**Fig.2** Experimental setup for the formation of a floating water bridge between two beakers filled with triply deionised water when a high voltage is applied. In this setup and all figures presented the anode beaker is at the right.

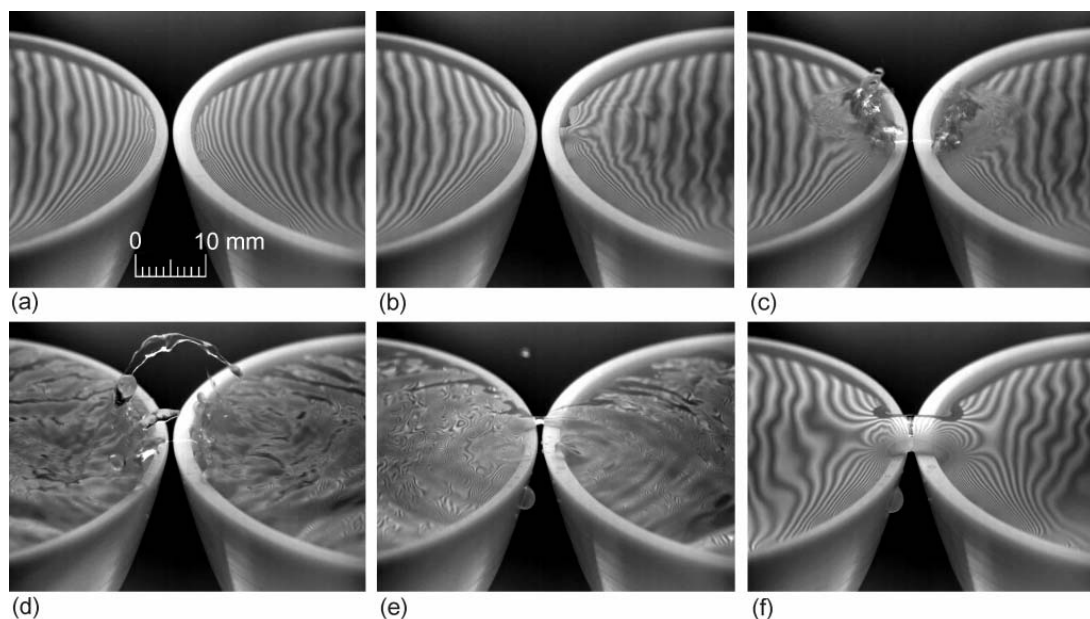


**Fig.3** Bridge formation between two Teflon beakers. The shape of the water surface is contoured by the distortions of the otherwise parallel line reflections. In b the high voltage was applied to the electrodes, in e a watery connection formed, in f the bridge was stabilized.

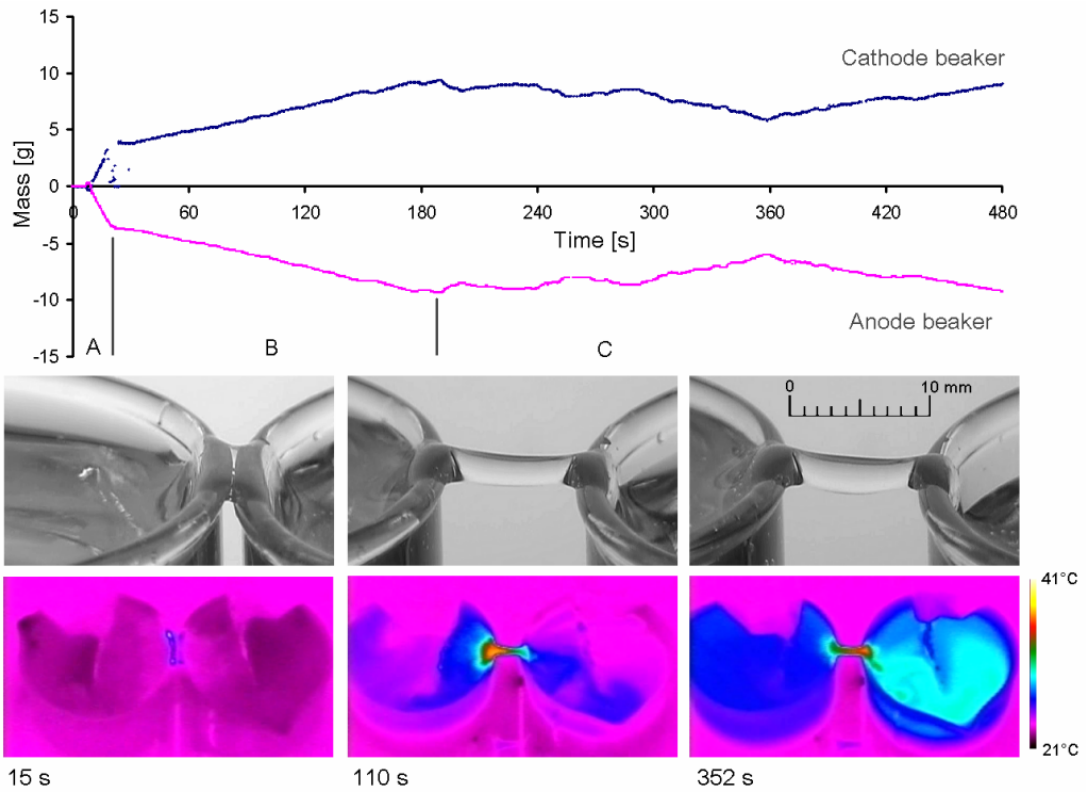


**Fig.4** Mass transport through the water bridge.

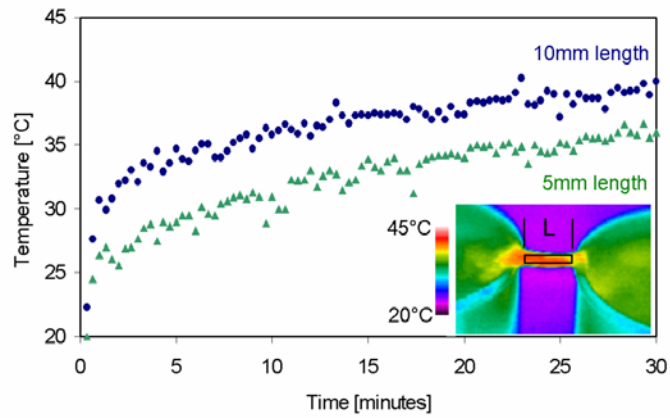


**Fig.5** Temperature increase on the bridge surface for bridges of 5mm and 10mm lengths (beaker to beaker distance L). The section averaged for the temperature measurement is indicated by a black square in the image.

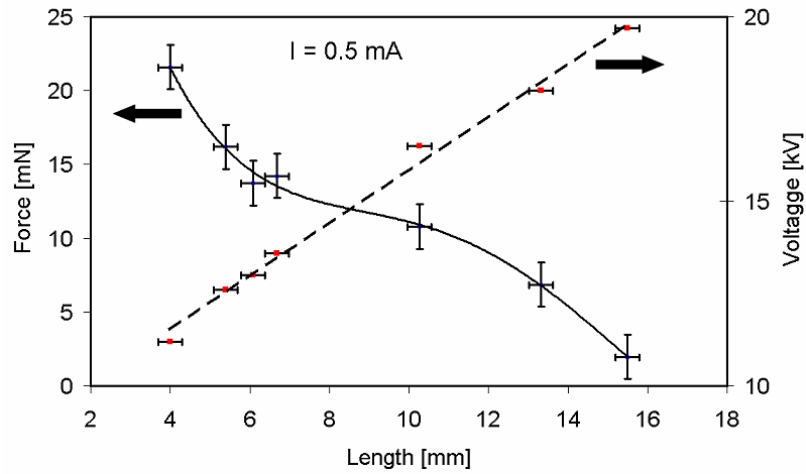


**Fig.6** Force between the two beakers as a function of the bridge length (beaker to beaker distance). Increasing the length also increased the voltage necessary to keep the current constant. The mid-length bridge diameter changed from 2.2 mm at 5 mm length to 1.6 mm diameter at 15 mm length.

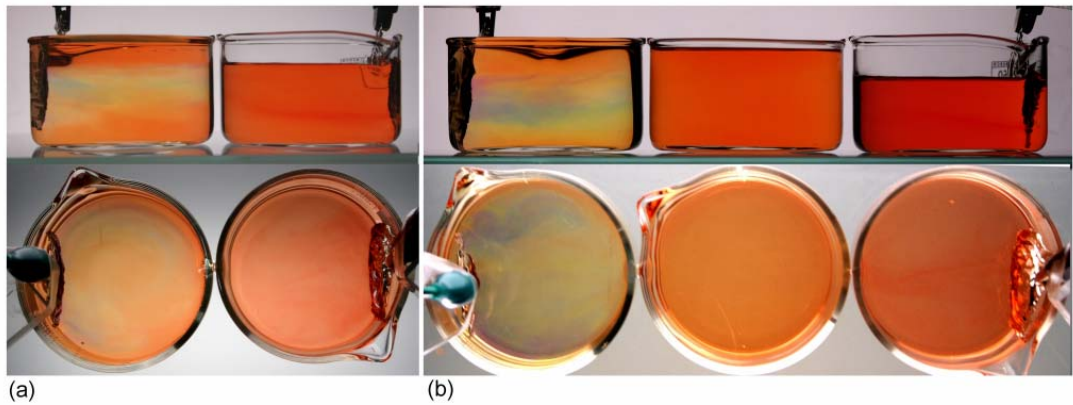


**Fig.7** Visualization of the pH value during bridge operation from red (pH 4) to violet (pH 10) for (a) a two beaker and (b) a three beaker arrangement. With orange pH 5, yellow pH 6, green pH 7, cyan pH 8 and blue pH 9. Before bridge operation the water had a pH value of 5 (orange). The colour impression also depends on the thickness of the water layer.

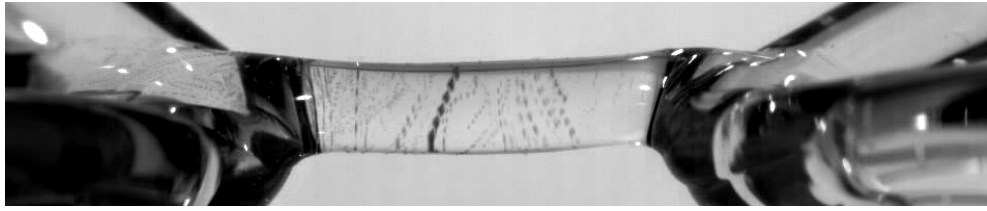


**Fig.8** Tracking of particles on the surface of a 1.6 mm thick water bridge. The interval between the single images was 1 ms. Particles imaged through the bridge appear as large dots. The rotational direction was clockwise when looking towards the cathode beaker (left).

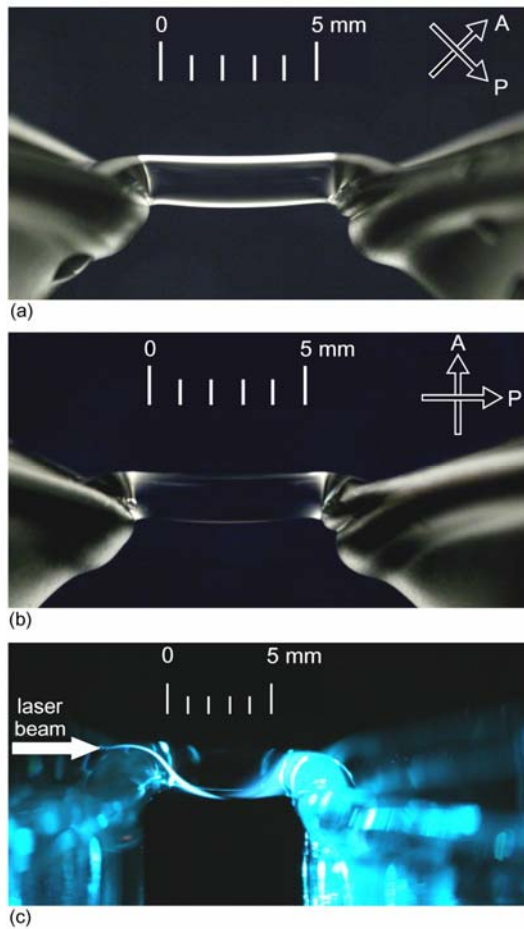


**Fig.9.** (a, b) The water bridge between two crossed linear polarizer plates. P indicates the direction of the polarizer, A the direction of the analyser. (c) shows a focused laser beam shining through the length of the bridge.

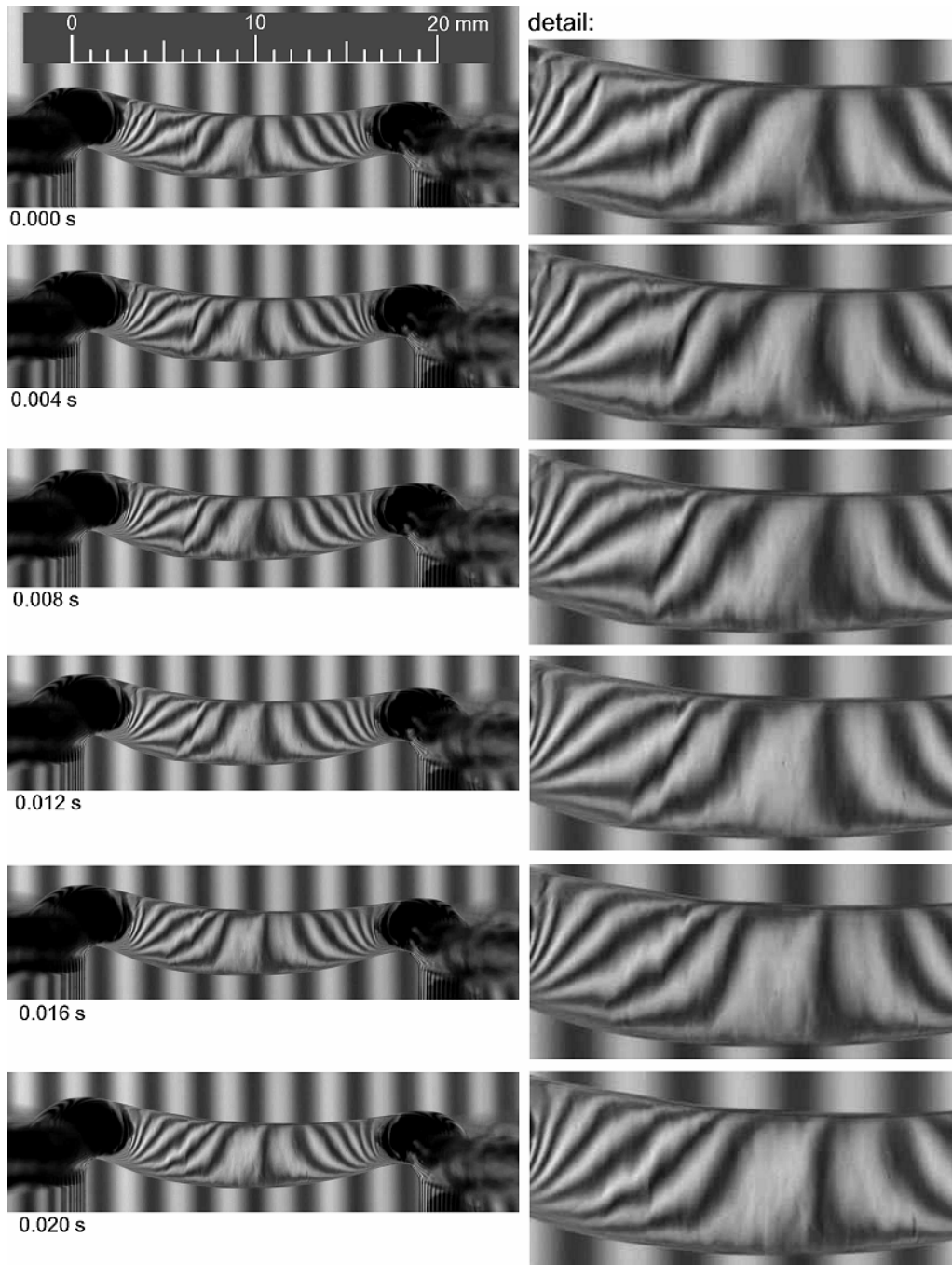


**Fig.10** Vertical grid lines imaged through the water bridge, in a series of frames from the high-speed camera.



**Fig.11** Deflection of the floating water bridge in the vicinity of a charged glass rod.